



Research Article

# Synthesis and Characterization of Copper Nanoparticle-coated Abaca (*Musa textilis*) Fibers for the Antibacterial and Mechanical Enhancement of Biodegradable Composite Films

Muhammad Adlim<sup>1,2\*</sup>, Lisa Aufia<sup>2</sup>, Yardina Azizah<sup>2</sup>, Ibnu Khaldun<sup>2</sup>, Abdul Gani<sup>2</sup>, Noor Hana Hanif Abu Bakar<sup>3</sup>, Muhammad Syukri Surbakti<sup>4</sup>, Noraini Ahmad<sup>5</sup>, Ismail Ozmen<sup>6</sup>, Subhan Salaeh<sup>7</sup>

<sup>1</sup>Graduate School of Mathematics and Applied Science, Universitas Syiah Kuala, Darussalam Banda Aceh, 23111, Indonesia

<sup>2</sup>Chemistry Department, Teacher Training and Education Faculty (FKIP), Universitas Syiah Kuala, Darussalam Banda Aceh, 23111, Indonesia

<sup>3</sup>School of Chemical Sciences, Universiti Sains Malaysia, 11800 USM, Penang, Malaysia

<sup>4</sup>Physics Department, Faculty of Mathematics and Natural Sciences (FMIPA), Syiah Kuala University, Darussalam Banda Aceh, 23111 Indonesia

<sup>5</sup>Department of Chemistry, Faculty of Science, Universiti Malaya, 50603 Kuala Lumpur, Malaysia

<sup>6</sup>Department of Chemistry, Faculty of Engineering and Nature Sciences, Suleyman Demirel University, Isparta, 32260, Turkey

<sup>7</sup>Faculty of Science and Technology, Prince of Songkla University, Pattani Campus, Pattani, 94000, Thailand

\*Corresponding author: [adlim@usk.ac.id](mailto:adlim@usk.ac.id); Tel.: 0651-7554229; Fax.: -

**Abstract:** Environmentally friendly and biodegradable composites are increasingly being studied for use in compatible films, safe food packaging, and wound dressings. Strengthening composite films with modified natural fibers has received limited attention. In this study, biodegradable composite films reinforced with abaca fibers coated with copper nanoparticles were successfully prepared. Copper nanoparticles (CuNPs) were incorporated to provide both antimicrobial and conductive properties. Copper nanoparticle-coated abaca (banana) fibers (CuNPs) were synthesized by the stepwise reduction method, in which the nanoparticles were first prepared and subsequently immobilized onto abaca fibers (AF). This method produced stronger treated fibers than those prepared using a simultaneous reduction method. CuNPs on the surface of PVA-coated AF are nanosized and well-dispersed particles, resulting in higher electrical conductivity compared with the control (PVA-AF only). The incorporation of CuNP-coated PVA-AF into the composite film matrix (containing PVA, tapioca starch, glycerol, and chitosan) significantly improved the tensile strength and elongation compared with the control film. The thickness of films containing higher PVA content (60%–80%) increased compared with those with lower PVA proportions. A similar trend was observed for the water absorption, tensile strength, and elongation properties. The antibacterial activity of CuNP-coated AF showed an inhibition zone of 14 mm, which was comparable to that of gentamicin (17 mm). However, the antibacterial effect was localized and did not diffuse throughout the film.

**Keywords:** Banana fibers; Copper nanoparticles; Conducting film; Polyvinyl alcohol; Tapioca

## 1. Introduction

Polyvinyl alcohol (PVA) is known as a nontoxic and biodegradable polymer, especially in ecosystems containing suitably acclimated microorganisms (Chiellini et al., 2003), and it has been claimed that the PVA-based detergent additive is safe for the environment; however, the claim is still controversial (Sustainablejungle.com, 2023). Studies on PVA blended with starch

and natural polymers have been conducted to enhance the biodegradability of the composite. PVA dissolves in warm water and has been used as a stabilizer for colloidal copper nanoparticles (Kanchana et al., 2023; El-Shamy, 2019). However, studies on impregnating colloidal copper nanoparticles with or without PVA on Abaca fiber (banana fibers) are not well-known.

The water miscibility and transparent properties of PVA provide advantages in film preparation, but the mechanical properties of PVA films are considered low (Peng and Chen, 2018). Tapioca starch was added to proportionally substitute some PVA content in the composite to increase biodegradability and reduce production cost. The abaca fibers and chitosan within the PVA composite film are expected to be more flexible and durable.

The literature elaborating nearly similar composite compositions has been reviewed (Asrofi et al., 2025; Rathinavel and Saravanakumar, 2021; Teli and Sheikh, 2013). Coating polyester yarn with copper oxide has been patented as upon, but colloidal copper particles on Abaca fibers, which are subsequently embedded in polyvinyl alcohol (PVA) composite film, remain unexplored. Conducting film has been popular in liquid crystal display (LCD) and photovoltaic technology. It is usually made of indium tin oxide (ITO) and coated with polyethylene terephthalate (PET) or polyethylene naphthalate (PEN). Since ITO is expensive, substituted materials have been intensively studied using graphene, carbon nanotubes, and other materials. However, substitute materials are still less cost-effective and require complicated procedures (Sharpe et al., 2024; Malvankar et al., 2012). Therefore, colloidal copper nanoparticle-coated abaca fiber would be a cost-effective alternative material. Conducting yarn is known in smart textile technology (McCann and Bryson, 2022). The yarn was coated with polyaniline (PANI) through an in situ polymerization technique (Hong et al., 2018). The copper-coated polyester yarn was prepared using a laser with the magnetron sputtering method (Peng and Chen, 2018).

This study introduces a new PVA composite film prepared by coating abaca fibers with copper nanoparticles and embedding them within a biodegradable PVA composite thin film, unlike most reported conducting films, in which the entire film area contains the conducting material. Abaca fibers are one of the strongest naturally occurring fibers. They are lightweight, flexible, and durable in saltwater (Araya-Gutiérrez et al., 2023). They are used to strengthen composite films. The insertion of copper-coated fibers within the PVA composite film is expected to generate moderate conduction. Copper nanoparticle-coated abaca fibers are designed to provide both antimicrobial and electrical conduction within the PVA composite film. The appropriate formula and characteristics of the new composite were studied. This study reported a new biodegradable composite with acceptable strength, moderate electrical conductivity, and antibacterial properties, which have wide potential applications in smart textiles, food packaging, agriculture, pharmacy, and electronics.

## 2. Methods

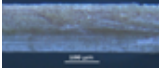


### 2.1 Material and Equipment used

Several research materials were used in this study. Abaca banana fibers (*Musa textilis*) were purchased from an online commercial supplier. Polyvinyl alcohol (Millipore, PA), copper (II) sulfate pentahydrate ( $\text{CuSO}_4 \cdot 5\text{H}_2\text{O}$ , ACS), ascorbic acid (99.0%), tapioca flour, glycerol (ACS), and chitosan (medium MW) were used. All chemicals were purchased from Merck, Singapore. The samples were characterized using instruments: optical microscopes (ZEISS Primostar). XRF (Panalytical Epsilon 3 XLE) was used to determine the chemical composition of the CuNPs. SEM (JEOL JSM-6360LA) scanned composite surface images. Mesdanlab Strength (Tensolab-5000) was used to analyze the mechanical strength. An Instex Dual Display Digital Multimeter (type GDM-8245) was used to measure the electrical conductance, and a TEM (JEOL JEM-1400, Japan) was used to obtain data on the CuNP particle morphology. FTIR spectroscopy (Shimadzu) was used to identify the functional groups before and after composite formation.

## 2.2 The Experimental Procedure

The entire experimental procedure is summarized in Table 1.

**Table 1** The sequence of research procedures is summarized in the following diagram:

1 →	2 →	3 →	4 →	5
Synthesis of Cu NPs & impregnation on Fiber <ul style="list-style-type: none"> <li>• stepwise</li> <li>• simultaneous</li> </ul> 	Characterizations: <ul style="list-style-type: none"> <li>• SEM</li> <li>• TEM</li> <li>• AAS</li> <li>• light microscope</li> <li>• FTIR</li> </ul>	Preparation of conductive biofilm <ul style="list-style-type: none"> <li>• Various composites</li> <li>• Controls</li> </ul> 	Chemical, physical & mechanical characterization <ul style="list-style-type: none"> <li>• XRF</li> <li>• Thinness</li> <li>• Water adsorption</li> <li>• Mechanical</li> <li>• Electrical</li> </ul>	Antibacterial analysis <ul style="list-style-type: none"> <li>• Controls</li> <li>• Cu-Fibers</li> <li>• Biofilm between Cu-fibers</li> </ul> 

### 2.2.1 Synthesis of CuNPs

An aqueous PVA solution (5 wt%) was prepared by dissolving 11 g of PVA powder in hot water (Ting and Sun, 2000) and diluting it to 220 mL. A 74 mL of 2.3 M  $CuSO_4 \cdot H_2O$  solution was slowly added to the PVA solution while stirring. Ascorbic acid solution (100 mL 1.9 M) was slowly added to the PVA-Cu solution while heating at 60°C, and the pH was neutralized by adding a few drops of NaOH (1.35 M). The solution was stirred using a magnetic stirrer for 2 hours. The solution was then left at room temperature for 2 days. The CuNPs were separated by centrifugation and washed several times using a mixture of 50% aqueous vinegar and 50% ethanol. The precipitate (Cu nanoparticles) was dried in an oven at 70°C for 2 h.

### 2.2.2 Stepwise and simultaneous in situ abaca fiber coating with PVA/Cu

Abaca fibers were cleaned and sorted into relatively uniform diameters with a total weight of  $\pm 20$  grams. The fibers (15 cm) were dipped into a tray containing 1% PVA solution and dried in an oven at 50°C. The coating procedure is repeated thrice to prepare three layers of the PVA film coating. For coating observation only, a different dye was added to the PVA solution at each layer for contrast. The coloring layer was done for visual characterization. The treated fibers were referred to as PVA-coated fibers.

PVA-coated fibers were coated with copper nanoparticles either stepwise or simultaneously. Stepwise method: the abaca fibers were dipped one by one into a tray containing colloidal copper nanoparticles and dried in an oven at 50°C. Simultaneous method: abaca fibers were mixed with copper ion-PVA solution as described (procedure 2.3.1) before the addition of acid. The treated fiber was identified as AF-PVA-Cu. As a comparison, instead of copper from solution (CuNPs), copper powder (ground with a ball mill) was also immobilized on AF-PVA with the stepwise method, which was then noted as AF-PVA-Cu<sub>powder</sub>. AF-PVA-Cu<sub>powder</sub> was only used in the comparison study of SEM, conductivity, and antibacterial activity.

### 2.2.3 Preparation of biodegradable PVA composite film with/without AF-PVA-Cu

The components of the biodegradable PVA composite film were blending in various proportion of tapioca flour, PVA, glycerol, and chitosan, as shown in Table 2. Tapioca flour is dissolved in distilled water with a 1:20 volume ratio of tapioca weight and water of 1:20 (1 g in 20 mL) until completely mixed (starch solution). Then, the tapioca solution was heated at 60-70°C while being stirred using a magnetic stirrer. PVA (in various weights) was dissolved in

220 mL of hot water and mixed with a tapioca solution. Glycerol (1 mL), chitosan (1 mL), and distilled water were slowly added to obtain 250 mL. The mixture was mixed and stirred for 30 minutes. The mixture was molded using a perpendicular mold (acrylic tray) and allowed to dry at room temperature for 3 x 24 hours. The film mold is 13 cm in length, 11.5 cm in width, and 0.5 cm in height. Before film drying, the fibers (AF-PVA-Cu) were arranged lengthwise on the base of the mold surface one by one at a distance of 1 cm. The dried film was removed from the mold, and its thickness was measured using a digital screw micrometer.

**Table 2** Biofilm composition of stepwise preparation

Sample Code	Tapioca (g)	PVA (g)	Glycerol (mL)	Chitosan (mL)	Abaca fibers	
					include	exclude
T0/P100-AF	0	2.5	0	0	✓	
T20/P80-AF	0.5	2.0	0	0	✓	
T20/P80/G-AF	0.5	2.0	1	0	✓	
T40/P60/G-AF	1.0	1.5	1	0	✓	
T60/P40/G-AF	1.5	1.0	1	0	✓	
T60/P40/G	1.5	1.0	1	0		✓
T20/P80/G-Cu	0.5	2.0	1	0	✓	
T40/P60/G-Cu	1.0	1.5	1	0	✓	
T60/P40/G-Cu	1.5	1.0	1	0	✓	
T60/P40/G/CH	1.5	1.0	1	1	✓	

Volume total; 250 mL

**Sample code:**

P100-AF : 100% PVA, PVA-coated abaca fiber

T20/P80-AF : Tapioca (20%), PVA (80%), PVA-coated abaca fiber

T20/P80/G-AF : Tapioca (20%), PVA (80%), glycerol, PVA-coated abaca fiber

T40/P60/G-AF : Tapioca (40%), PVA (60%), glycerol, PVA-coated abaca fiber

T60/P40/G-AF : Tapioca (60%), PVA (40%), glycerol, PVA-coated abaca fiber

T60/P40/G : Tapioca (60%), PVA (40%), glycerol

T20/P80/G-Cu : Tapioca (20%), PVA (80%), glycerol, PVA-Cu coated abaca fiber

T40/P60/G-Cu : Tapioca (40%), PVA (60%), glycerol, PVA-Cu coated abaca fiber

T60/P40/G-Cu : Tapioca (40%), PVA (60%), glycerol, PVA-Cu coated abaca fiber

T60/P40/G/CH : Tapioca (40%), PVA (60%), glycerol, chitosan, PVA-coated abaca fiber

## 2.2.4 Characterization of Cu-Fiber Biofilm Composites

The copper nanoparticle powder was analyzed using X-ray fluorescence (XRF) and FTIR. The AF-PVA-Cu (coated fiber) was analyzed using scanning electron microscopy (SEM), transmission electron microscopy (TEM), optical microscope, AAS, and FTIR. The conductivity and mechanical properties of the composite were analyzed. The water absorption test was performed based on the ASTM D570-98 procedure with slight modifications. The samples were cut into 1x1 cm sizes, then weighed and dipped in water for 1 min (Judawisastra et al., 2017). The remaining water on the sample surface was dried using a napkin and reweighed. The tensile strength and elongation of biofilms were measured using the Mesdanlab Strength machine type tensolab 5000. The sample was prepared and verified using the ASTM D638 test specimen. The tensile strength value was calculated using Equation 1 :

$$\sigma = \frac{F_{\max}}{A} \quad (1)$$

where:

$\sigma$  = Tensile strength (N/mm<sup>2</sup>)

$F_{\max}$  = maximum stress (N)

$A$  = surface area (mm<sup>2</sup>)

The percentage of elongation can be determined using Equation 2 (Handayani & Nurzanah, 2018) :

$$\varepsilon = \frac{\Delta L}{L_0} \times 100\% \quad (2)$$

where:

$\varepsilon$  = elongation (%)

$\Delta L$  = ( $L - L_0$ ) increase in length (mm)

$L_0$  = initial length (mm)

An Instek Dual Display Digital Multimeter type GDM-8245 was used to measure the electrical conductivity of AF-PVA-Cu and controls (AF, PVA, and AF-PVA without Cu). The test device was set to the resistance ( $\Omega$ ) measurement mode. The fiber sample to be measured was prepared by placing the fiber on a straight and tense support. The measuring probe was then connected to each end of the fiber whose conductivity would be measured with a distance of 10 cm. The electrical conductivity value ( $\sigma\Omega$ ) for each sample was calculated using Equation 3 (Alves et al., 2022):

$$\sigma = \frac{L}{R \times A} \quad (3)$$

where:

$\sigma$  = conductivity value of the material (S/cm)

$L$  = length of material (cm)

$R$  = resistance value of the material ( $\Omega$ )

$A$  = surface area of the material (cm<sup>2</sup>)

The data obtained from the thickness and water absorption tests were analyzed using one-way analysis of variance (ANOVA), followed by Duncan's test with a significance level of  $p \leq 0.05$ .

### 2.2.5 Antibacterial Test

The glassware was sterilized using alcohol and dried in an oven at 180°C for 2 hours. The inoculating loops were directly flamed over a burner, and the calibrated glassware was autoclaved at 121°C for 15 minutes (Dhuha, 2016). Nutrient Agar (NA, 8.4 g) was dissolved in 300 mL of distilled water, heated while stirring until homogeneous. It was then sterilized using an autoclave at 121°C for 15 minutes (Fusieger et al., 2022). The solution was cooled to approximately 40°C before being poured into sterile Petri dishes ( $\pm 20$  mL per dish) and then allowed to cool and solidify (Zamilah et al., 2020). The tested microbe was *E. coli*, which was rejuvenated by transferring a loopful of the bacteria into a slant NA medium, followed by incubation at 37°C for 24–48 h in an incubator (Berliana and Pujiyanto, 2020). A loopful of the rejuvenated *E. coli* was suspended in 10 mL of 0.9% NaCl physiological solution and then incubated at 37°C for 24 hours (Menamo et al., 2017).

The antibacterial activity test was conducted using the well diffusion method. A 24-hour-old bacterial suspension was prepared equivalent to 0.5 McFarland standard. This suspension was mixed with MHA medium until it was well distributed (Berliana and Pujiyanto, 2020). Wells with a diameter of 6 mm were aseptically made in the agar. Samples were fiber-coated CuNPs (chemically synthesized), PVA thin film composite with or without chitosan (taken area between fiber-coated copper), and some controls (fiber only, PVA film only, fiber-coated copper powder prepared with ball-milled nano preparation). Samples were cut into small fragments, filled in circularly, and transferred into each well. The inhibition zone in millimeters represents areas where bacterial growth was inhibited (Badr, 2018).

### 3. Results and Discussion

#### 3.1 Synthesis and Characterization of CuNPs

During CuNP synthesis, the solution changed from blue to light green, dark green, brownish, and red, indicating copper formation (Figure 1). The color change from blue to green was a mixture of copper ions (blue) and partially oxidized ascorbic acid (yellow). The reaction mechanism involved the formation of  $\text{Cu}(\text{OH})_2$ , which was then reduced by ascorbic acid into  $\text{Cu}_2\text{O}$ , and ascorbic acid was oxidized into dehydroascorbic acid (Reaction 1) (Barrita and Sánchez, 2013).  $\text{Cu}_2\text{O}$  was then further oxidized by the rest of the ascorbic acid, and finally, Cu was formed (reaction 2) (Liu et al., 2012):

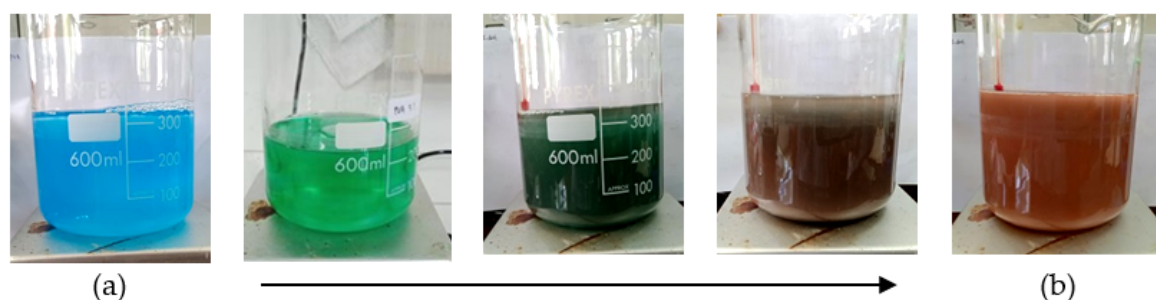
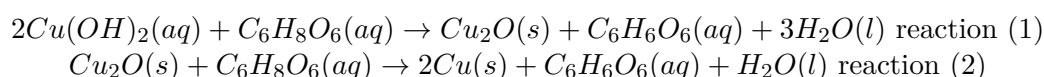


**Figure 1** Color changes during CuNPs synthesis; (a) PVA +  $\text{Cu}^{2+}$ ; (b) equivalent addition of ascorbic with  $\text{Cu}^{2+}$  and formation of CuNPs

Abaca fibers (AF) were mixed with the initial solution in the simultaneous coating method (Figure 1a) so that copper ions were stuck on the fibers before being reduced into CuNPs (Figure 1b). However, the AF-PVA-Cu fibers became fragile; therefore, we focused only on the stepwise method, where CuNPs were prepared first and then the powder was immersed and immobilized on the fibers, so that corrosive chemicals did not contact the fibers.

The XRF data of CuNPs confirmed the formation of copper metal, reaching a proportion of up to 99.5% compared to the trace metals. Among the oxides, CuO dominated up to 99.8%, as shown in Table 3. CuO exists because copper metal, especially in nanosized particles, is easily oxidized into CuO in an open atmosphere (Esmail et al., 2021).

**Table 3** X-ray fluorescence data of the dried copper nanoparticle powder

Element			Oxide		
Composition	Concentration	Unit	Composition	Concentration	Unit
Al	0.108	%	$\text{Al}_2\text{O}_3$	0.000	ppm
P	0.273	%	$\text{P}_2\text{O}_5$	0.000	%
Cu	99.461	%	CuO	99.826	%
Ca	0.114	%	CaO	0.132	%

#### 3.2 PVA-coated AF and its characterization

The PVA coating on the AF cross-section confirmed three layers: red, yellow, and blue (outer layer), as shown in Supplement-1. Abaca fibers coated with 1%, 5%, and 10% PVA gave layers of 46.918, 101.332, and 109.372  $\mu\text{m}$ , respectively. The coating was stable after drying because the PVA acted as an adhesive with hydroxyl groups (Nasrollahzadeh, 2021). The higher the PVA concentration, the stronger the adhesive properties; however, the coated abaca fibers will stick to each other. Therefore, PVA (1%) fulfilled the required characteristics.

### 3.3 Copper impregnation on PVA-AF and its characterization

#### 3.3.1 Surface analysis of PVA-coated AF impregnated with CuNPs (AF-PVA-Cu)

The surface characterization of AF-PVA-Cu fibers using an optical microscope with 40x magnification differentiates the fibers coated with commercial Cu powder from those coated with CuNPs (Figure 2 a-b). As shown in Figure 2a, the commercial Cu powder coating appeared to have large aggregated particles on the AF surface. While the surface of the CuNPs coating appeared fine, dispersed particles covered the entire fiber surface (Figure 2b), and the layers are illustrated in Figure 2c. Nano-sized particles have a more uniform size, allowing for intensive interaction with the surrounding environment. CuNPs synthesized through the chemical reduction method usually have a size range of 126-375 nm (Manjunath et al., 2016; Liu et al., 2012).

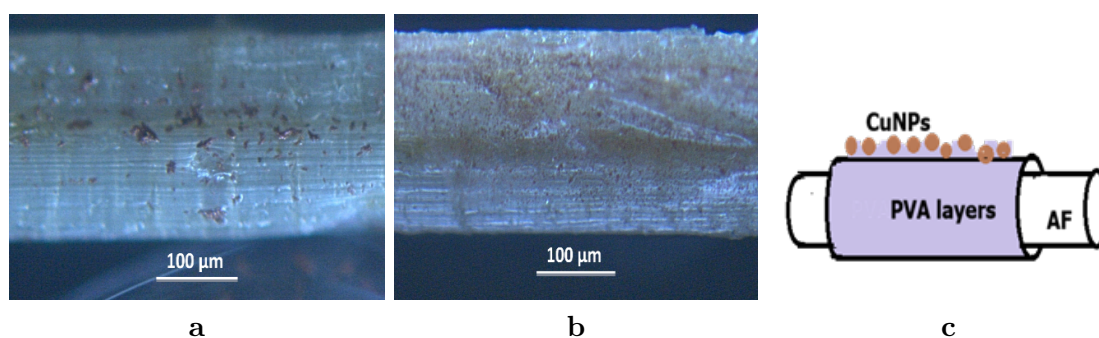


**Figure 2** Microscope images (40x magnification) of AFs coated with polyvinyl alcohol and impregnated with (a) commercial Cu-powder; (b) CuNPs with 40x magnification; (c) illustrated layers

The cross-section SEM images of PVA-coated AF impregnated with CuNPs show a rough and hollow surface at 500x magnification, as shown in Figure 3 (a), and the detailed structures, including the pores and morphology of PVA-Cu-NPs composite, are shown in Figure 3 (b). This coating characteristic contributes to the AF composite's physical properties, including water absorption and mechanical strength.

Figure 4 shows the SEM images of PVA-coated AF with CuNPs impregnation and control. The PVA-coated AF without CuNPs (control) showed a rough surface with longitudinal strips (Figure 4a), whereas the PVA-coated AF impregnated with CuNPs was covered with CuNPs spread throughout the fiber surface (Figure 4b). At higher magnification (5000x, Figure 4c, and 40000x magnification, Figure 5d), the CuNP clusters were trapped in the PVA matrix, and the CuNP clusters agglomerated into  $\sim 5 \mu\text{m}$ . The CuNP surface looks rough compared to the previously reported CuO/Cu<sub>2</sub>O-coated cellulose fibers (Tomsic et al., 2022).

#### 3.3.2 Particle size of CuNPs in PVA-AF-Cu Composites

The PVA-AF-Cu composite was immersed in water, and the copper particle size was recorded using transmission electron microscopy. Several TEM images (Figure 5a) were analyzed with the "ImageJ" application ([www.imagej.net](http://www.imagej.net)) to measure particle diameters and distribution, as shown in Figure 5b. The particles were dispersed with a narrow size distribution. Nearly all the particles have a uniform particle size of around 10-30 nm, as shown in Figure 5. The PVA protected the CuNPs from aggregation and kept them in nanosize. Immobilization on the AF shall provide copper nanoparticles on natural fiber, which are compatibly embedded in a biocomposite and biodegradable film.

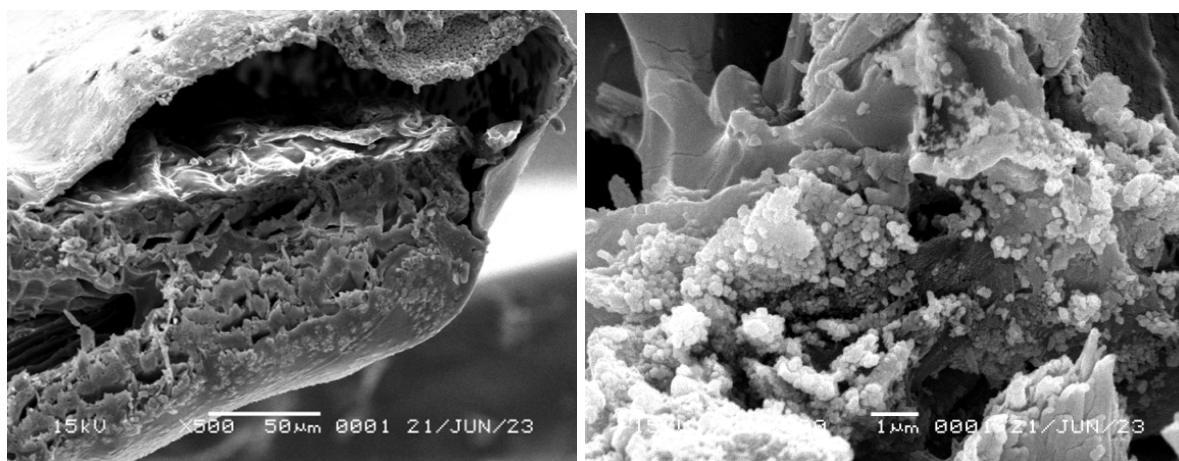


**Figure 3** SEM images of the cross-section of PVA-coated AF immobilized with CuNPs (a) 500x magnification; (b) 10,000x magnification

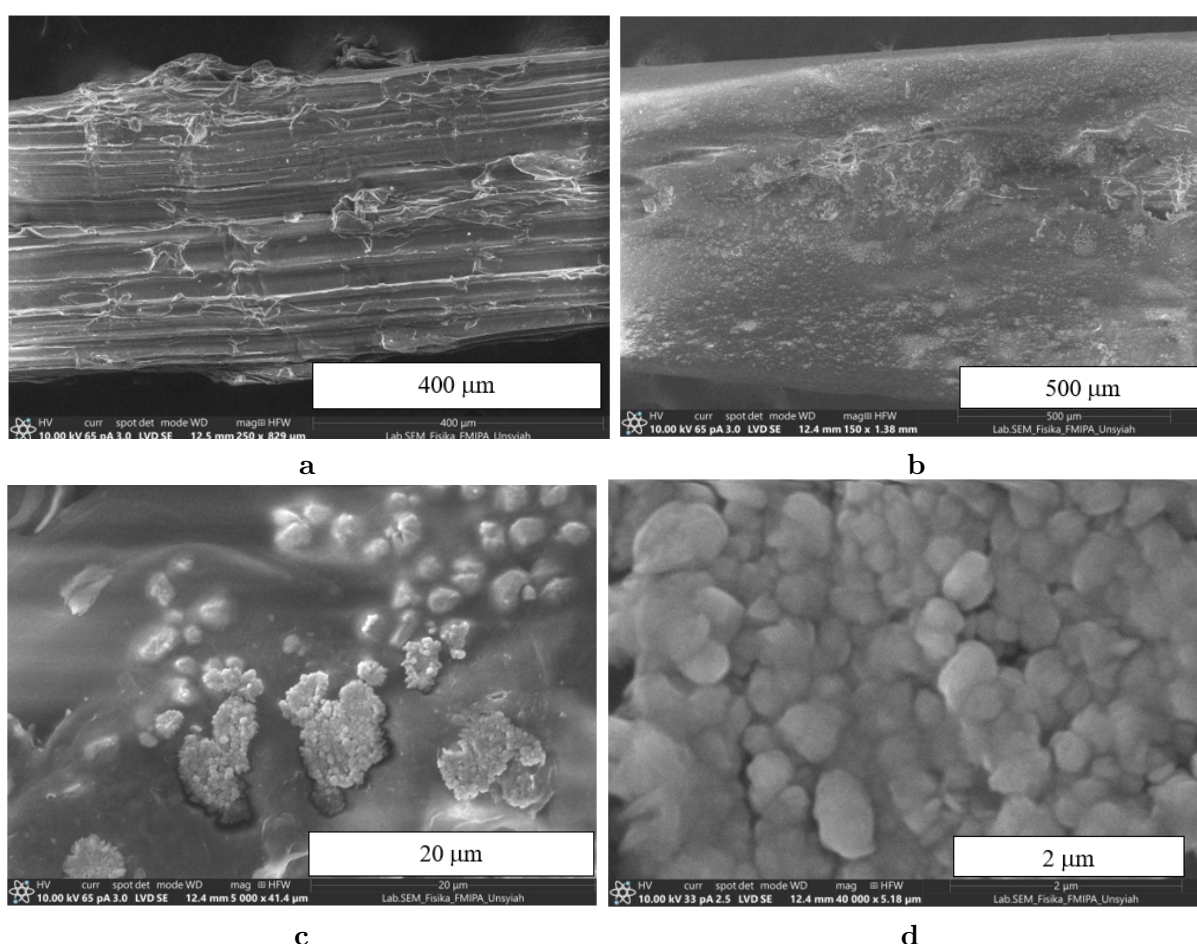


**Figure 4** SEM images of the outer surface of PVA-coated AF (a) without CuNP impregnation (250x magnification, control); (b) with CuNP impregnation (150x magnification); (c) at 5000x magnification; (d) at 40000x magnification

### 3.3.3 Electrical Conductivity of PVA-AF-Cu Composites

The electrical resistance of the PVA-coated AF with and without copper impregnations and the control were compared, as shown in Table 4. The electrical resistance is the reciprocal of the conductance. The conductivity of the PVA-coated fiber sample (PVA-AF) is lower than that of the fiber without coating (AF only) because it experiences additional resistance. The

PVA-coated AF with Cu impregnation (PVA-AF-CuNPs) shows higher conductivity than those without CuNPs (PVA-AF only), which is  $5.568 \times 10^{-5}$  S/cm, respectively. and  $4.503 \times 10^{-5}$  S/cm. The impregnation of CuNPs increases the conductivity of the composite. However, the conductivity was insignificant compared with that of a copper wire of the same size, which is  $6.622 \times 10^{-2}$  S/cm. This phenomenon was due to copper oxidation and impregnation's homogenization effect. The CuO compound has lower conductivity than pure Cu and is classified as a semiconductor material. CuO is a p-type semiconductor with a bandgap of 1.3-2.1 eV at room temperature. Previous research reported that the conductivity of PVA doped by CuO was  $27^{\circ}\text{C}$  is  $5.7 \times 10^{-7}$  S/cm, which is lower than that of PVA-AF-CuNPs.

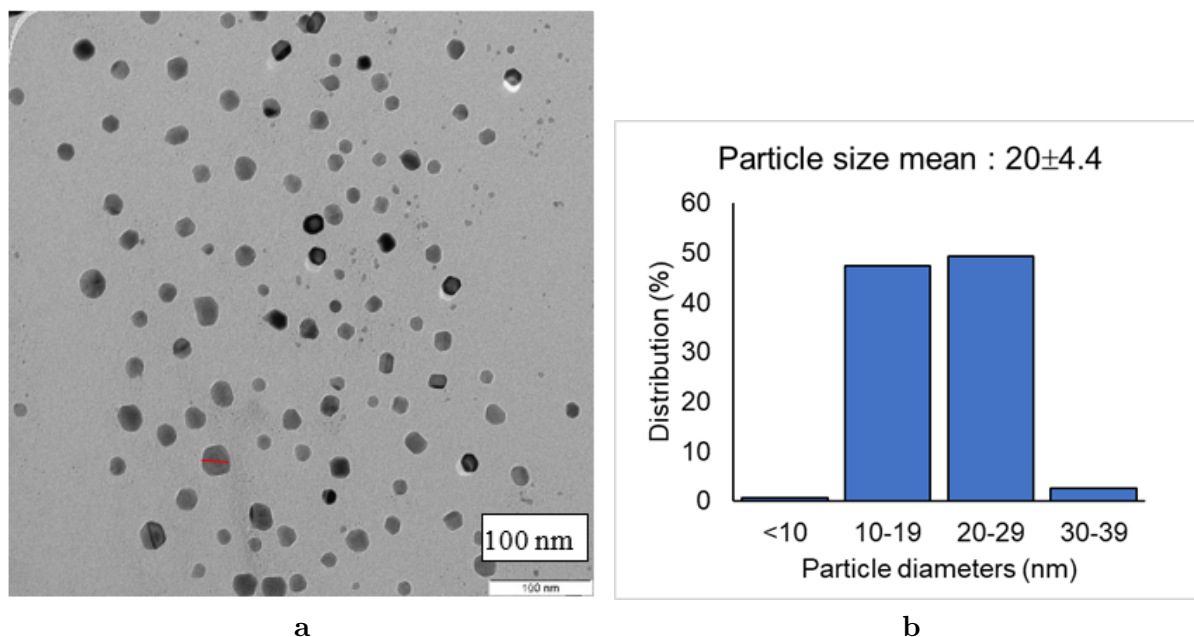


**Figure 5** (a) Representative transmission electron microscopy image of CuNPs (scale bar : 100 nm) released from PVA-AF-Cu composites, (b) particle distribution

**Table 4** Conductance of PVA-AF-CuNPs compared to controls

Sample	d (cm)	L (cm)	R( $\Omega$ )	$\sigma$ (S/cm)
Just AF (fiber)	0.183	10	345900	$5.032 \times 10^{-5}$
PVA-AF	0.183	10	386500	$4.503 \times 10^{-5}$
PVA-AF-CuNPs	0.183	10	312600	$5.568 \times 10^{-5}$
Copper wire	0.100	10	0.0483	$6.622 \times 10^{-2}$

where:

d = material diameter (cm)

L = material length (cm)

R = resistance ( $\Omega$ )

$\sigma$  = electrical conductivity (S/cm)

### 3.4 PVA-AF-CuNPs embedded in biodegradation composite film (PVA-Tapioca-glycerol-chitosan)

#### 3.4.1 BCF thickness

The composition of biodegradable composite films affects their characteristics. BCF containing tapioca, PVA, and glycerol, excluding PVA-AF-CuNPs embedding, was used as a control sample (Figure 6a). BCF is an elastic transparent film and is denoted as [T60/P40/G]. Tapioca

(T) and PVA (P) composition with AF represented by [T0/P100-AF] and [T20/P80-AF]. The effect of glycerol was deduced from the [T20/P80/G-AF] and [T20/P80/G-AF] samples. The influence of PVA-AF-CuNP embedding (Cu) within the BCF was studied from [T60/P40/G] and [T60/P40/G-Cu], and the image is presented in Figure 6b. Figure 6c is similar to the sample in Figure 6b, except that the film composition contains chitosan. Table 2 presents all content combinations. Glycerol-containing samples are more elastic and softer than those without glycerol. All BCFs were uniform in size and printed in the same mold; however, the higher the PVA content, the thicker the BCFs, as measured with a digital screw micrometer at three points, as shown in Table 5. The influence of PVA content on film properties is consistent with a previous study (Aminingsih et al., 2021).

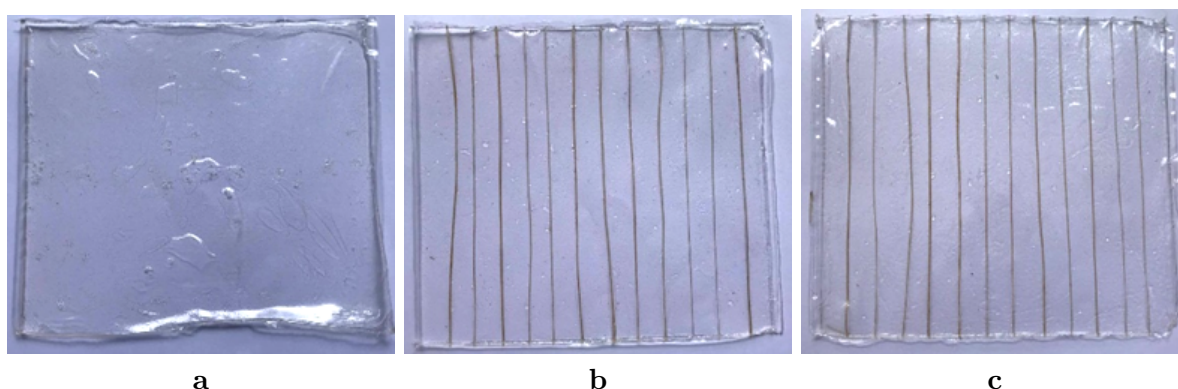


**Figure 6** Representative image of BCFs: (a) without embedded AF-PVA-CuNPs, (b) with embedded AF-PVA-CuNPs, and (c) with AF-PVA-CuNPs and chitosan

PVA forms a larger porous structure than starch because of its higher hydrophilicity and ability to form hydrogen bonds with water. This allows PVA to absorb water more effectively and create a larger and more open pore structure than starch; thus, samples with high PVA content formed a thicker film. In addition, PVA has a high molecular weight and strong intermolecular forces, which contribute to the formation of a stable foam structure. Strong intermolecular forces between PVA chains allow for the formation of strong hydrogen bonds, which help stabilize the foam structure and prevent collapse or shrinkage. Starch, on the other hand, has limited solubility in water and tends to form aggregates or clumps during dispersion, making foam structures less stable.

**Table 5** Thickness of BCFs with various compositions

No.	Sample Code	Biofilm Thickness (mm)
1	T0/P100-AF	$0.087 \pm 0.015^a$
2	T20/P80-AF	$0.097 \pm 0.015^{ab}$
3	T20/P80/G-AF	$0.167 \pm 0.059^c$
4	T40/P60/G-AF	$0.157 \pm 0.012^c$
5	T60/P40/G-AF	$0.130 \pm 0.020^{abc}$
6	T60/P40/G	$0.150 \pm 0.010^c$
7	T20/P80/G-Cu	$0.163 \pm 0.012^c$
8	T40/P60/G-Cu	$0.140 \pm 0.035^{bc}$
9	T60/P40/G-Cu	$0.130 \pm 0.020^{abc}$
10	T60/P40/G/CH	$0.143 \pm 0.006^{bc}$

*Remarks:* a, b, c, d = statistically significantly different, data with similar subscript labels are insignificantly different

Glycerol also has a significant effect on the BCF thickness. The [T20/P80/G-AF] is significantly thicker than the [T20/P80-AF]. The thicknesses of BCFs are classified according to the Japanese Industrial Standard, which indicates that a good biofilm thickness should be  $<0.25$

mm (Brilianti et al., 2023).

### 3.4.2 FTIR studies of the BCFs

The chemical functional groups within the BCF were studied using the FTIR method, as shown in Figure 7. The interaction of copper ions with PVA has been reported previously (Raju et al., 2007). The hydroxyl band appears at  $3436\text{ cm}^{-1}$  in BCF only and shifts to  $3427\text{ cm}^{-1}$  in BCF containing CuNPs. The absorption bands at  $1400\text{ cm}^{-1}$  in the BCF sample and at  $1407\text{ cm}^{-1}$  in the Cu composite indicate the presence of carbonate ions, which are a common inorganic ion group (Nandiyanto et al., 2019).

The primary and secondary alcohol groups represent bands of  $1019\text{ cm}^{-1}$  and  $1028\text{ cm}^{-1}$ , respectively. Carbonyl groups with a band at  $1572\text{ cm}^{-1}$  in composite biofilms containing CuNPs suggest that the involvement of carboxylic acid in the synthesis changes the dehydroascorbic acid structure (Nandiyanto et al., 2019).

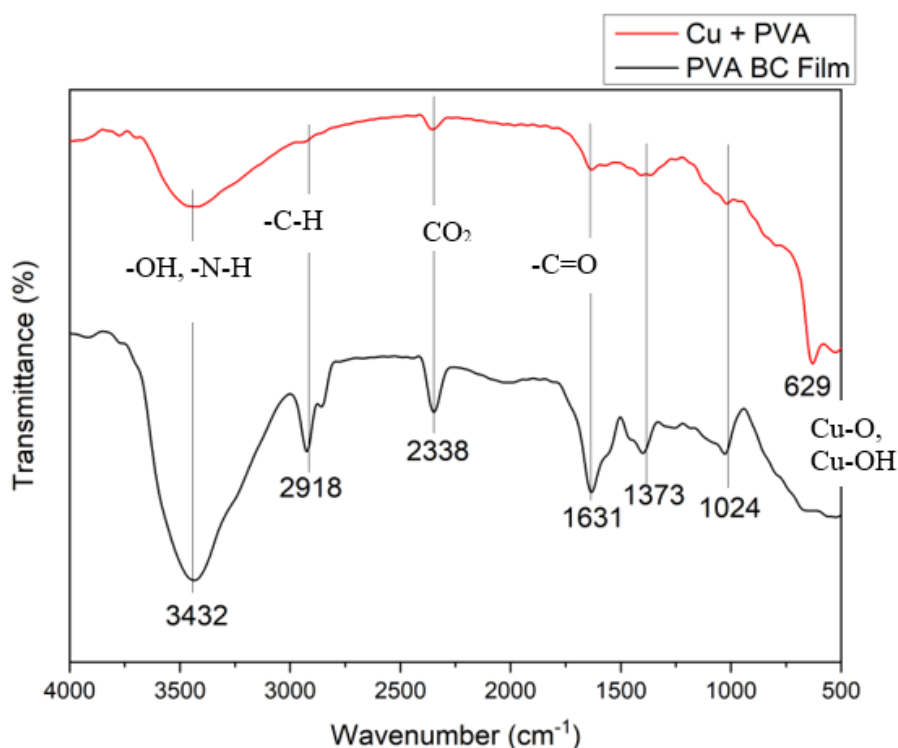


**Figure 7** FTIR comparison between CuNPs and PVA biodegradable composite film, a new band at  $629\text{ cm}^{-1}$  indicated the existence of Cu-O and Cu-OH as an interaction Cu-PVA within the sample

Figure 7 shows new absorption peaks (at  $629\text{ cm}^{-1}$ ) representing Cu-O and Cu-OH bonds due to the chemical interaction between PVA and ascorbic acid with Cu during the synthesis process. The FTIR Cu-O characteristic peaks confirm the previous report (Duman et al., 2016). Cu-OH band of  $3774$  and  $3697\text{ cm}^{-1}$  implies stretching vibrations of the -OH group (Machiril et al., 2017). Other bands, including  $2900\text{ cm}^{-1}$  (C-H stretching),  $3000\text{-}3500\text{ cm}^{-1}$  (O-H stretching), and  $1600\text{-}1700\text{ cm}^{-1}$  (O-H bending), were also observed, and the FT-IR characteristics were verified (Ali et al., 2018).

### 3.4.3 Water absorption capacity

The capacity of BCF to absorb water from the environment is one of its important properties. Hydrophilic components of BCF tend to interact and bind with water molecules, forming hydrogen bonds (Ismail and Zaaba, 2011). However, the preferred property of BCF is its moderate water absorption capacity. When BCF has a water content  $> 10\%$ , it will be biodegradable

but easily decomposes in a moist environment. Table 6 lists the water absorption capacities in minute water immersion of the BCF.

**Table 6** Water Absorption of BCFs

No.	Sample Code	Water Absorption Capacity (%)
1	T0/P100-AF	$96.67 \pm 5.8^c$
2	T20/P80-AF	$84.54 \pm 4.7^b$
3	T20/P80/G-AF	$71.67 \pm 1.8^a$
4	T40/P60/G-AF	$115.14 \pm 3.5^{ef}$
5	T60/P40/G-AF	$126.92 \pm 4.9^g$
6	T60/P40/G	$127.66 \pm 5.4^g$
7	T20/P80/G-Cu	$88.65 \pm 7.1^{ab}$
8	T40/P60/G-Cu	$105.56 \pm 5.6^d$
9	T60/P40/G-Cu	$121.43 \pm 7.1^{fg}$
10	T60/P40/G/CH	$106.48 \pm 2.6^{de}$

*Remarks:* data labelled with similar superscript alphabet are insignificantly different at  $\alpha = 0.05$

Table 6 shows that the BCF absorbs a large amount of water. Tapioca enhances water absorption. The amylose within tapioca tends to form hydrogen bonds with water, causing high water absorption (Hambali et al., 2020). BCF with a composition of 20% tapioca and 80% PVA with the addition of glycerol (T20/P80/G-Cu) is recommended. The percentage of water absorption of the biofilm obtained in this study was between 71.67-127.66%, which is lower than the characteristics of the PVA-tapioca film in a previous study (Judawisastra et al., 2017).

#### 3.4.4 Tensile strength and elasticity

The strength of BCFs was measured by the extent to which a material can withstand pressure and tension before breaking. High tensile strength indicates durable and strong BCFs. Figure 8 shows that the BCF tensile strengths were 60.70–82.96 MPa, which is classified as acceptable based on the Indonesian National Standard (SNI) and JIS, where bioplastic standard tensile strength ranges from 24.7-302 Mpa (Brilianti et al., 2023). The highest tensile strength value is found in the T40/P60/G-AF sample of 82.96 MPa, while the lowest tensile strength is found in the T20/P80/G-Cu sample of 60.70 MPa. AF without CuNPs increased the BCF durability, but CuNPs reduced BCF tensile strength because CuNPs still brought some corrosive chemicals from the salt precursor and the reducing agent (ascorbic acid) into the PVA-AF-CuNPs.

Figure 8 shows that BCF elongation increased when a combination of a high proportion of PVA and the presence of glycerol was used, as shown in T20/P80/G-Cu and T20/P80/G-AF, but the reverse trend was observed in T20/P80-AF (no glycerol). This is because PVA has a more flexible chemical structure and polymer chain. PVA addition disrupts the intermolecular bond structure in the tapioca matrix. This made the biofilm more flexible but with less mechanical strength. PVA has a long amorphous chain that is flexible and elastic because it can undergo plastic deformation. Tapioca has a more fragile structure because it has a polysaccharide chain that produces a rigid crystalline structure (Li et al., 2000). The tensile strength of biofilms increased significantly with the addition of 1% CuNPs but decreased with the addition of 2% and 3% CuNPs (Sharma et al., 2021). This is because the addition of filler allows agglomeration to form, which reduces the tensile strength.

The higher the PVA composition, the higher the elongation value, which is common in PVA-starch biofilms, indicating phase separation (Akbar et al., 2019). Meanwhile, biofilms with glycerol addition show a smaller amount of agglomeration. The addition of glycerol smoothens the surface and reduces clumping. This is because there is an interaction between glycerol

molecules and PVA, which can weaken the intermolecular bonds of PVA, thereby reducing the biofilm stiffness (Syamani et al., 2020). The biofilm with 100% PVA produced the highest elongation value (6.07%) compared with the composite with 50% PVA content, which has an elongation of 3.43%.

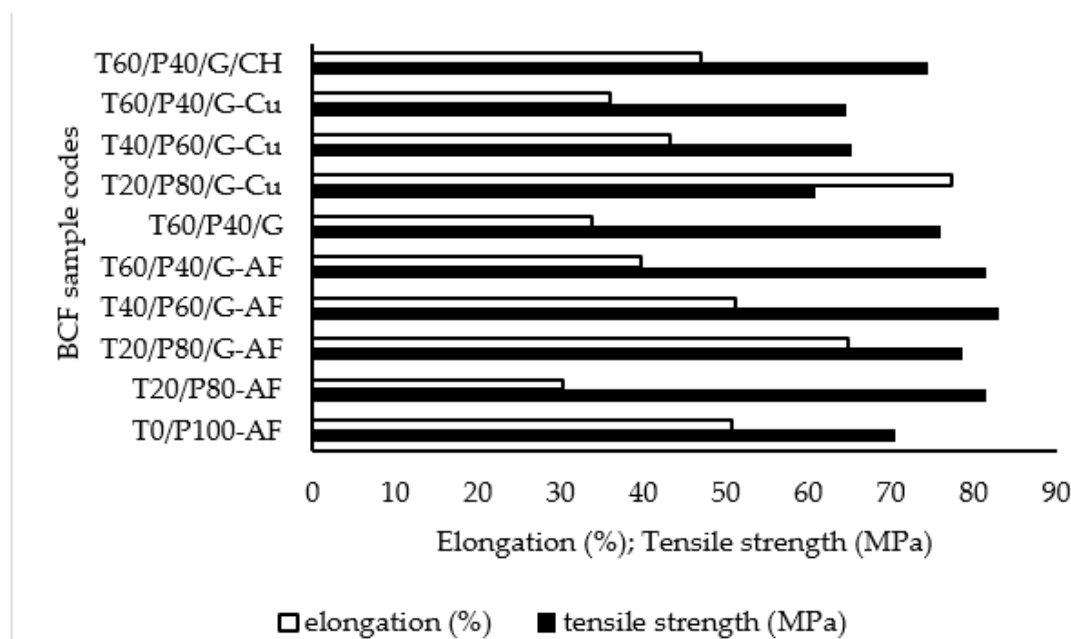


**Figure 8** Elongation and tensile strength of the BCFs

Elongation testing was also carried out on variations without abaca fiber; T60/P40/G as a control, and variations of T60/P40/G/CH with chitosan addition. Unlike the chitosan effect, the addition of AF did not affect the composite elongation parameter, as shown in T20/P80/G/CH. The elongation value of the biofilm in this study ranged from 30.29% to 77.31%. The elongation value produced from this study is classified as acceptable when compared to the Indonesian National Standard (SNI). According to SNI, the elongation value of bioplastics ranges from 21 to 220% (Brilianti et al., 2023).

### 3.4.5 Antibacterial properties

The antibacterial test was conducted not only on the coated fibers (AF) but also on the area between them, as illustrated in Supplement material-2. The properties were compared with the controls (AF only, PVA-coated fibers, PVA film only, and PVA biofilm composite). AF is the negative control that cannot inhibit the growth of *E. coli*. PVA-coated AF-Cu-powder was used as a positive control for comparison with PVA-coated AF-CuNPs. Most of the tests were in 3 replications.

Table 7 summarizes the bacterial inhibition zones for each sample, and the visual images are presented in Supplemental Material-3. PVA-coated AF containing either CuNPs or copper powder exhibited higher bacterial inhibition zones (11.40-14.65 mm) compared with other samples and controls, and was categorized as intermediate (Rahmadeni et al., 2019). The antibacterial activities of PVA-coated AF-Cu-powder > PVA-coated AF-Cu-NPs are due to the quantity of Cu-powder > CuNPs. The antibacterial activities of PVA-coated AF-Cu did not diffuse into other parts of the composite. This is deduced from the PVA biofilm sample taken between the composite fibers, which has a zero inhibition zone. Chitosan enhances the antibacterial activity of PVA-coated AF-Cu powder from 11.40 to 12.24 mm. Chitosan (trace component) did not exhibit prominent antibacterial activity, unlike copper, which dominated the composition. Copper activity is slightly lower than that of gentamicin (antibacterial standard tested on *E. coli*), which has an inhibition zone of 17 mm, as previously reported (Husen and Ratnaningtyas,

2022). Although the antibacterial properties of copper are known, CuNP-coated AF embedded in BFC has been introduced in the current studies. CuNPs penetrate *E. coli* cells and exert cytotoxicity by generating reactive oxygen species (ROS) within the cells. It can also replace or bind native cofactors of enzymes (metalloprotein) (Ma et al., 2022).

**Table 7** Summaries of inhibition zones of BFCs

NO	Samples	Inhibition zone (mm)			Mean (mm)
		Repl-1	Repl-2	Repl-3	
1.	Coated fiber (PVA-AF-CuNPs)	11.02	11.50	11.70	11.40
2.	PVA Biofilm PVA only (control)	0	0	0	0
3.	Sampled BCF between coated fiber (PVA-AF-CuNPs)	0	0	0	0
4.	PVA Biofilm only + Glycerol (control)	0	0	0	0
5.	Coated fiber (PVA-AF-Cu-powder) as K+ (positive control)	14.43	14.63	14.89	14.65
6.	AF only as K- (negative control)	0	0	0	0
7.	Coated fiber (PVA-AF-CuNPs)+chitosan	12.46	12.14	12.12	12.24
8.	Sampled BCF between coated fiber (PVA-AF-CuNPs) + chitosan	0	0	0	0
9.	PVA-AF + chitosan (control)	0	0	0	0
10.	Sampled BCF between coated fiber (PVA-AF+chitosan control)	0	0	0	0

Copper zero valent ( $\text{Co}^0$ ) and copper oxide kill *E. coli* bacteria in several ways.  $\text{Co}^0$  adheres to *E. coli* due to the opposite electrical charge, and chemical reduction occurs in the *E. coli* cell wall, causing damage (Raffi et al., 2010). Another possible cause is that  $\text{Cu}^0$  can be oxidized into  $\text{CuO}$  or  $\text{Cu}_2\text{O}$ , generating a Fenton-like reaction in the case of copper. Copper ions interact with water/peroxide in bacterial cells, and then produce reactive oxygen species, as superoxide radicals, which attack the bacterial DNA (Borkow and Gabbay, 2005).

As expected, the BCF containing PVA-coated AF-Cu-NPs confirmed that the copper particles are nanoscale. The CuNPs have been provided as a coat for abaca fibers instead of in powder form, which has wider applications. PVA functioned as a compatible stabilizer for CuNPs and as an adhesive to abaca fibers. The appropriate composition of PVA-tapioca-glycol-chitosan made the composite film flexible, biodegradable, and compatible with CuNP-coated abaca fibers. Embedding AF-Cu-NPs in the film composite (BCF) made BCF a stronger film with antimicrobial and conductive properties.

#### 4. Conclusions

This study demonstrates that direct in situ immobilization of CuNPs onto abaca fibers is structurally detrimental because the fibers degrade under corrosive synthesis conditions. A stepwise immobilization strategy was therefore developed to preserve fiber integrity while enabling homogeneous CuNP deposition on PVA-coated fibers. This approach ensured stable nanoparticle anchoring and effective interfacial compatibility within the polymer matrix. The incorporation of CuNPs significantly enhanced the electrical conductivity of PVA-AF composites compared to CuNP-free counterparts, confirming the functional contribution of the copper. The physico-mechanical properties of biodegradable composite films (BCF) composed of PVA, tapioca starch, and glycerol were predominantly governed by PVA content. Increasing PVA concentration (60–80 wt%) resulted in improved film thickness, water absorption capacity, tensile strength, and elongation at break, indicating enhanced polymer chain interactions and structural cohesion. All prepared films complied with Indonesian biofilm standards. Embedding PVA-AF-CuNPs into the BCF matrix exhibited notable antibacterial activity (inhibition zone:

12–14 mm), attributable to the presence of CuNPs. However, this antibacterial functionality did not translate to the bulk BCF, suggesting restricted nanoparticle mobility and limited diffusion within the film matrix. Overall, this study establishes a viable immobilization pathway for integrating conductive and antibacterial CuNPs onto natural fibers while enhancing the mechanical performance of biodegradable composite films. The findings provide a foundation for the development of multifunctional, sustainable materials for potential applications in active packaging and advanced biopolymer composites.

### Acknowledgements

This work was supported by Universitas Syiah Kuala Penelitian Profesor research funding: grant number 61/UN11.2.1/PG.01.03/SPK/PTNBH/2024 3rd May 2024. The Bridging grant (304/PKIMIA/6316598) from Universiti Sains Malaysia partially funded this research.

### Author Contributions

Research ideas and design (Muhammad Adlim), laboratory works (Lisa Aufia, Yardina Azizah), lab supervision (Ibnu Khaldun, Abdul Gani, M. Syukri Surbakti), typical sample characterization (Noor Hana Hanif Abu Bakar), publication guidance proofreading (Noraini Ahmad, Subhan Salaeh, Ismail Ozmen).

### Conflict of Interest

The authors declare that they have no known competing financial interests or personal relationships that could have appeared to influence the work reported in this paper.

### Supplementary Materials

Three figures are provided in the Supplemental Material

### References

- Akbar, M. F., Amri, A., & Zultiniar. (2019). Pembuatan bioplastik berbasis pati ubi jalar dan polyvinyl alcohol (PVA) menggunakan graphene sebagai filler dan gliserol sebagai plasticizer. *Jurnal Online Mahasiswa Fakultas Teknik*, 6, 1–10. <https://jom.unri.ac.id/index.php/JOMFTEKNIK/article/view/24215/23445>
- Ali, Z. I., Ghazy, O. A., Meligi, G., Saleh, H. H., & Bekhit, M. (2018). Radiation-induced synthesis of copper/poly(vinyl alcohol) nanocomposites and their catalytic activity. *Advances in Polymer Technology*, 37(2), 365–375. <https://doi.org/10.1002/adv.21675>
- Alves, Z., Ferreira, N. M., Ferreira, P., & Nunes, C. (2022). Design of heat sealable starch-chitosan bioplastics reinforced with reduced graphene oxide for active food packaging. *Carbohydrate Polymers*, 29, 1–11. <https://doi.org/10.1016/j.carbpol.2022.119517>
- Aminingsih, T., Heliawati, L., & Fathurrahman, M. (2021). Optimization of the addition of polivinil alcohol (PVA) as a plasticizer in biofilm with tapioca-chitosan flour material. *Helium: Journal of Science and Applied Chemistry*, 1(1), 30–36. <https://doi.org/10.33751/helium.v1i1.2954>
- Araya-Gutiérrez, D., Garro Monge, G., Jiménez-Quesada, K., Arias-Aguilar, D., & Quesada Cordero, R. (2023). Abaca: A general review on its characteristics, productivity, and market in the world. *Revista Facultad Nacional de Agronomía Medellín*, 76(1), 1–12. <https://doi.org/10.15446/rfnam.v76n1.101710>
- Asrofi, M., Asyari, N. A., Pradiza, R. R., Abduh, M., Yusuf, M., Mahardika, M., Ilyas, R. A., Asyraf, M. R. M., Sapuan, S. M., Knight, V. F., & Norrahim, M. N. F. (2025). Enhancing mechanical and thermal properties of PVA-abaca fiber biocomposites via ultrasonic vibration bath treatment. *Results in Engineering*, 25, 1–7. <https://doi.org/10.1016/j.rineng.2025.103935>

- Badr, A. A. (2018). Anti-microbial and durability characteristics of socks made of cotton and regenerated cellulosic fibers. *Alexandria Engineering Journal*, 57(4), 3367–3373. <https://doi.org/10.1016/j.aej.2017.11.015>
- Barrita, J. L. S., & Sánchez, M. D. S. S. (2013). Antioxidant role of ascorbic acid and his protective effects on chronic diseases. In *Intech* (pp. 449–484). <https://doi.org/10.5772/52181>
- Berliana, H., & Pujiyanto, S. (2020). Analisis efektivitas probiotik di dalam produk kecantikan sebagai antibakteri terhadap *Staphylococcus epidermidis*. *Berkala Bioteknologi*, 3(2), 24–30. <https://ejournal2.undip.ac.id/index.php/bb/article/view/9657>
- Borkow, G., & Gabbay, J. (2005). Copper as a biocidal tool. *Current Medicinal Chemistry*, 12(18), 2163–2175. <https://doi.org/10.2174/0929867054637617>
- Brilianti, K. F., Ridlo, A., & Sedjati, S. (2023). Sifat mekanik dan ketebalan bioplastik dari *Kappaphycus alvarezii* menggunakan variasi konsentrasi amilum dengan plemastis gliserol. *Journal of Marine Research*, 12(1), 95–102. <https://doi.org/10.14710/jmr.v12i1.34169>
- Chiellini, E., Corti, A., D'Antone, S., & Solaro, R. (2003). Biodegradation of poly(vinyl alcohol) based materials. *Progress in Polymer Science*, 28(6), 963–1014. [https://doi.org/10.1016/S0079-6700\(02\)00149-1](https://doi.org/10.1016/S0079-6700(02)00149-1)
- Dhuha, S. (2016). Aktivitas antibakteri ekstrak etanol daun lamun (*Syringodium isoetifolium*) terhadap bakteri *Pseudomonas aeruginosa*. *Pharmacoin*, 5(1), 231–237. <https://doi.org/10.35799/pha.5.2016.11246>
- El-Shamy, A. G. (2019). Composite (PVA/Cu nano) films: Two yield points, embedding mechanism, and thermal properties. *Progress in Organic Coatings*, 127, 252–259. <https://doi.org/10.1016/j.porgcoat.2018.11.024>
- Esmail, R. T. E., Golshan, M., Kalajahi, M. S., & Mamaqani, H. R. (2021). Synthesis of copper and copper oxide nanoparticles with different morphologies using aniline as reducing agent. *Solid State Communications*, 1–9. <https://doi.org/10.1016/j.ssc.2021.114364>
- Fusieger, A., da Silva, R. R., de Jesus Silva, S. R., Honorato, J. A., Teixeira, C. G., Souza, L. V., Magalhães, I. N. S., da Silva Costa, N. A., Walter, A., Nero, L. A., Caggia, C., & de Carvalho, A. F. (2022). Inhibitory activity of an emulsifying salt polyphosphate (JOHA HBS®) used in processed cheese: An in vitro analysis of its antibacterial potential. *Food Science and Technology*, 167, 1–10. <https://doi.org/10.1016/j.lwt.2022.113777>
- Hambali, E., Suryani, A., Rivai, & Permadi, P. (2020). *Teknologi surfaktan dan aplikasinya* (Edisi Revisi). IPB Press. <https://fliphtml5.com/qycnc/vpwj>
- Hong, J., Han, X., Shi, H., Jin, L., & Yao, J. (2018). Preparation of conductive silk fibroin yarns coated with polyaniline using an improved method based on in situ polymerization. *Synthetic Metals*, 235, 89–96. <https://doi.org/10.1016/j.synthmet.2017.12.002>
- Husen, F., & Ratnaningtyas, N. I. (2022). Inhibitory test of gentamicin antibiotics against *Escherichia coli* and *Staphylococcus aureus* bacteria using disc method. *Biotropika: Journal of Tropical Biology*, 10(2), 126–131. <https://doi.org/10.21776/ub.biotropika.2022.010.02.06>
- Ismail, H., & Zaaba, N. F. (2011). Effect of additives on properties of polyvinyl alcohol (PVA)/tapioca starch biodegradable films. *Polymer-Plastics Technology and Engineering*, 50(12), 1214–1219. <https://doi.org/10.1080/03602559.2011.566241>
- Judawisastra, H., Sitohang, R. D. R., & Marta, L. (2017). Water absorption and its effect on the tensile properties of tapioca starch/polyvinyl alcohol bioplastics. *IOP Conference Series: Materials Science and Engineering*, 223(1), 1–9. <https://iopscience.iop.org/article/10.1088/1757-899X/223/1/012066>
- Kanchana, S. K., Vanitha, N., & Basavaraj, R. B. (2023). Structural and optical properties of polyvinyl alcohol/copper oxide (PVA/CuO) nanocomposites. *Solid State Communications*, 370, 115221. <https://doi.org/10.1016/j.ssc.2023.115221>

- Li, H., Zhang, W., Xu, W., & Zhang, X. (2000). Hydrogen bonding governs the elastic properties of poly(vinyl alcohol) in water: Single-molecule force spectroscopic studies of PVA by AFM. *Macromolecules*, *33*(2), 465–469. <https://doi.org/10.1021/ma990878e>
- Liu, Q. M., Yasunami, T., Kuruda, K., & Okido, M. (2012). Preparation of Cu nanoparticles with ascorbic acid by aqueous solution reduction method. *Transactions of Nonferrous Metals Society of China*, *22*(9), 2198–2203. [https://doi.org/10.1016/S1003-6326\(11\)61449-0](https://doi.org/10.1016/S1003-6326(11)61449-0)
- Ma, X., Zhou, S., Xu, X., & Du, Q. (2022). Copper-containing nanoparticles: Mechanism of antimicrobial effect and application in dentistry – a narrative review. *Frontiers in Surgery*, *9*, 905892. <https://doi.org/10.3389/fsurg.2022.905892>
- Malvankar, N. S., Lau, J., Nevin, K. P., Franks, A. E., Tuominen, M. T., & Lovley, D. R. (2012). Electrical conductivity in a mixed-species biofilm. *Applied and Environmental Microbiology*, *78*(16), 5967–5971. <https://doi.org/10.1128/AEM.01803-12>
- Manjunath, A., Irfan, M., Anushree, K. P., Vinutha, K. M., & Yamunarani, N. (2016). Synthesis and characterization of CuO nanoparticles and CuO doped PVA nanocomposites. *Advances in Materials Physics and Chemistry*, *6*(10), 263–273. <https://doi.org/10.4236/ampc.2016.610026>
- McCann, J., & Bryson, D. (2022). *Smart clothes and wearable technology* (Second Edition). Woodhead Publishing. <https://doi.org/10.1016/B978-1-84569-357-2.50024-1>
- Menamo, D. S., Ayele, D. W., & Ali, M. T. (2017). Green synthesis, characterization, and antibacterial activity of copper nanoparticles using L-ascorbic acid as a reducing agent. *Ethiopian Journal of Science and Technology*, *10*(3), 209–220. <https://doi.org/10.4314/ejst.v10i3.5>
- Nandiyanto, A. B. D., Oktiani, R., & Ragadhita, R. (2019). How to read and interpret FTIR spectroscopy of organic material. *Indonesian Journal of Science and Technology*, *4*(1), 97–118. <https://doi.org/10.17509/ijost.v4i1.15806>
- Nasrollahzadeh, M. (2021). *Biopolymer-based metal nanoparticle chemistry for sustainable applications*. Susan Dennis. <https://doi.org/10.1016/B978-0-323-89970-3.00002-0>
- Peng, C., & Chen, G. (2018). Preparation and assessment of heat-treated  $\alpha$ -chitin nanowhiskers reinforced poly(vinyl alcohol) film for packaging application. *Materials*, *11*(10), 1–11. <https://doi.org/10.3390/ma11101883>
- Raffi, M., Mehrwan, S., Bhatti, T. M., Akhter, J. I., Hameed, A., Yawar, W., & Hasan, M. M. (2010). Investigations into the antibacterial behavior of copper nanoparticles against *Escherichia coli*. *Annals of Microbiology*, *60*(1), 75–80. <https://doi.org/10.1007/s13213-010-0015-6>
- Rahmadeni, Y., Febria, F. A., & Bakhtiar, A. (2019). Potensi Pakih Sipasan (*Blechnum orientale*) sebagai antibakteri terhadap *Staphylococcus aureus* dan Methicillin resistant *Staphylococcus aureus*. *Metamorfosa: Journal of Biological Sciences*, *6*(2), 224–229. <https://doi.org/10.24843/metamorfosa.2019.v06.i02.p12>
- Raju, C. H. L., Rao, J. L., Reddy, B. C. V., & Brahmam, A. K. V. (2007). Thermal and IR studies on copper doped polyvinyl alcohol. *Bulletin of Material Science*, *30*(3), 215–218.
- Rathinavel, S., & Saravanakumar, S. S. (2021). Development and analysis of poly vinyl alcohol/orange peel powder biocomposite films. *Journal of Natural Fibers*, *18*(12), 2045–2054. <https://doi.org/10.1080/15440478.2019.1711285>
- Sharma, B., Sandilya, A., Sharma, S., Garg, M., & Sadhu, S. D. (2021). Thermo-mechanical investigation of PEG–PVA biohybrid active film grafted with copper nanoparticles for packaging applications. *Bulletin of Materials Science*, *44*(2), 1–11. <https://doi.org/10.1007/s12034-021-02363-z>
- Sharpe, R. K., Quijada, M., Terrones, M., & Rana, M. M. (2024). Thin conducting films: Preparation methods, optical and electrical properties, and emerging trends, challenges, and opportunities. *Materials*, *17*(18), 1–140. <https://doi.org/10.3390/ma17184559>
- Sustainablejungle.com. (2023, November). What is PVA (or polyvinyl alcohol) and how environmentally friendly is it? [13 November]. <https://www.sustainablejungle.com/what-is-pva/>

- Syamani, F. A., Kusumaningrum, W. B., Akbar, F., Ismadi, Widyaningrum, F., & Pramasari, D. A. (2020). Characteristics of bioplastic made from modified cassava starch with addition of polyvinyl alcohol. *IOP Conference Series: Earth and Environmental Science*, 591(1), 1–7. <https://doi.org/10.1088/1755-1315/591/1/012016>
- Teli, M. D., & Sheikh, J. (2013). Modified bamboo rayon–copper nanoparticle composites as antibacterial textiles. *International Journal of Biological Macromolecules*, 61, 302–307. <https://doi.org/10.1016/j.ijbiomac.2013.07.015>
- Ting, Y. P., & Sun, G. (2000). Use of polyvinyl alcohol as a cell immobilization matrix for copper biosorption by yeast cells. *Journal of Chemical Technology and Biotechnology*, 75(7), 541–546. [https://doi.org/10.1002/1097-4660\(200007\)75:7<541::AID-JCTB247>3.0.CO;2-9](https://doi.org/10.1002/1097-4660(200007)75:7<541::AID-JCTB247>3.0.CO;2-9)
- Tomsic, B., Markovic, D., Jankovic, V., Simoncic, B., Nikodinovic-Runic, J., Ilic-Tomic, T., & Radetic, M. (2022). Biodegradation of cellulose fibers functionalized with CuO/Cu<sub>2</sub>O nanoparticles in combination with polycarboxylic acids. *Cellulose*, 29, 287–302. <https://doi.org/10.1007/s10570-021-04296-6>
- Zamilah, M., Ruhimat, U., & Setiawan, D. (2020). Media alternatif kacang tanah untuk pertumbuhan bakteri. *Journal of Indonesian Medical Laboratory and Science*, 1(1), 57–65. <https://doi.org/10.53699/joimedlabs.v1i1.11>